Genetic and functional characterization of clonally derived adult human brown adipocytes

Kosaku Shinoda[1,2,3,12], **Ineke H N Luijten**[1,2,3,4,12], **Yutaka Hasegawa**[1,2,3], **Haemin Hong**[1,2,3], **Si B Sonne**[1,2,3,11], **Miae Kim**[1,2,3,11], **Ruidan Xue**[5,6], **Maria Chondronikola**[7,8,9,10], **Aaron M Cypess**[5,6], **Yu-Hua Tseng**[5,6], **Jan Nedergaard**[4], **Labros S Sidossis**[7,8,9,10], and **Shingo Kajimura**[1,2,3]

[1]Diabetes Center, University of California, San Francisco (UCSF), San Francisco, California, USA

[2]Department of Cell and Tissue Biology, UCSF, San Francisco, California, USA

[3]Eli and Edythe Broad Center of Regeneration Medicine and Stem Cell Research, UCSF, San Francisco, California, USA

[4]Department of Molecular Biosciences, The Wenner-Gren Institute, Stockholm University, Stockholm, Sweden

[5]Joslin Diabetes Center, Boston, Massachusetts, USA

[6]Harvard Medical School, Boston, Massachusetts, USA

[7]Metabolism Unit, Shriners Hospitals for Children, Galveston, Texas, USA

[8]Department of Internal Medicine, University of Texas Medical Branch, Galveston, Texas, USA

[9]Department of Surgery, University of Texas Medical Branch, Galveston, Texas, USA

[10]Department of Nutrition and Metabolism, University of Texas Medical Branch, Galveston, Texas, USA.

Abstract

Brown adipose tissue (BAT) acts in mammals as a natural defense system against hypothermia, and its activation to a state of increased energy expenditure is believed to protect against the

development of obesity. Even though the existence of BAT in adult humans has been widely appreciated[1–8], its cellular origin and molecular identity remain elusive largely because of high cellular heterogeneity within various adipose tissue depots. To understand the nature of adult human brown adipocytes at single cell resolution, we isolated clonally derived adipocytes from stromal vascular fractions of adult human BAT from two individuals and globally analyzed their molecular signatures. We used RNA sequencing followed by unbiased genome-wide expression analyses and found that a population of uncoupling protein 1 (UCP1)-positive human adipocytes possessed molecular signatures resembling those of a recruitable form of thermogenic adipocytes (that is, beige adipocytes). In addition, we identified molecular markers that were highly enriched in UCP1-positive human adipocytes, a set that included potassium channel K3 (*KCNK3*) and mitochondrial tumor suppressor 1 (*MTUS1*). Further, we functionally characterized these two markers using a loss-of-function approach and found that *KCNK3* and *MTUS1* were required for beige adipocyte differentiation and thermogenic function. The results of this study present new opportunities for human BAT research, such as facilitating cell-based disease modeling and unbiased screens for thermogenic regulators.

Recent studies using ^{18}fluoro-2-deoxyglucose positron emission tomography (^{18}FDG-PET) scanning demonstrated that the prevalence of adult human BAT is inversely correlated with body mass index (BMI), adiposity, and fasting plasma glucose level[1–6], indicating that BAT is likely to play a role in human metabolism. Current evidence indicates that two types of UCP1-positive thermogenic adipocytes exist in rodents and humans: classical brown adipocytes and beige adipocytes (also known as brite adipocytes). Classical brown adipocytes arise from a subset of the dermomyotome during embryonic development[9–12]. They are found predominantly in adipose depots of rodents and infants that are mostly dedicated to BAT, such as those in the interscapular regions. Beige adipocytes, on the other hand, reside mainly in subcutaneous white adipose tissues (WAT), where they arise postnatally in response to certain external cues—such as chronic cold exposure or long-term treatment with agonists of peroxisome proliferator-activated receptor-γ (PPAR-γ)—a process often referred to as the 'browning' of WAT[13–17].

Although previous studies have reported that adult human BAT possesses a molecular signature resembling that of mouse beige adipocytes[16,18,19], more recent data imply that cultured adipocytes derived from adult human BAT express several classical brown adipocyte–selective markers that were originally found in mice[20]. This discrepancy appears to be primarily due to a few reasons. First, adult human BAT is a highly heterogeneous tissue compared to mouse BAT, consisting of UCP1-positive multilocular brown adipocytes, UCP1-negative unilocular white adipocytes, endothelial cells, stromal cells, and immune cells. Indeed, the gene-expression profile of human BAT in the neck region varies depending on the depth of the tissue[21]. Hence, molecular analyses of biopsied adult human BAT samples could be confounded by potential contamination from UCP1-negative cells such as white adipocytes and myocytes. Second, conclusions made in previous studies were entirely based on the mRNA-expression profiles of a few selected genes that were originally identified in mice. Global and unbiased molecular analyses in a homogeneous cell population are therefore warranted to clarify the nature of adult human BAT. The discrepancy regarding the cellular identity of adult human BAT needs to be critically

assessed to make it possible to strategize future therapeutic interventions for anti-obesity treatment through targeting this tissue. Namely, the identification of human-specific BAT molecular markers will allow for the development of cell type–selective activators that are likely to act more effectively and more safely than non-specific activators in recruiting new thermogenic adipocytes, especially in subjects who do not possess appreciable levels of existing BAT. For example, even though non-selective pharmacological activation of the sympathetic nervous system via beta3-adrenoceptor agonists can activate both classical brown adipocytes and beige adipocytes, adverse effects on the cardiovascular system prevents the clinical use of these agonists[22].

To this end, we have isolated a total of 65 clonally immortalized preadipocyte lines from stromal vascular fractions (SVFs) obtained from UCP1-positive supraclavicular BAT biopsies of two non-obese individuals[20]. We found seven clonal lines (10.8%) among the clones isolated from these biopsies that exhibited highly adipogenic properties. This result was similar to that of a previous report showing that approximately 6.5% of cloned SVFs (20 out of 305 clonal lines) displayed adipogenic properties in culture[16]. We subsequently analyzed three out of the seven adipogenic lines for RNA sequencing (RNA-seq) and bioinformatics analyses. We also examined *UCP1* mRNA expression of the seven adipogenic clones in response to cAMP and to rosiglitazone (Supplementary Fig. 1a,b).

In order to study and identify the gene signatures of clonal brown adipocytes, we experimentally differentiated the three clonal preadipocyte cell lines into brown adipocytes under an adipogenic culture condition. We took this approach because it is not possible to immortalize clonally isolated brown adipocytes directly from human biopsy material because adipocytes are post-mitotic cells. These experimentally derived brown adipocytes cannot be formally construed as a cell line (that is, they cannot be serially passaged while maintaining their differentiated state), so we refer to them here as brown adipocyte cultures 1–3. Additionally, because matched WAT pairs from the same subjects were not available, we isolated 35 clonal preadipocyte lines from SVFs of subcutaneous WAT from a lean BMI-matched individual as a control, using the same immortalization protocol as for the brown preadipocyte lines to avoid potential contamination from SV40 large T antigen–mediated immortalization. The clonally derived preadipocyte lines from subcutaneous WAT were differentiated under the same cultured conditions as the clonal brown adipocyte cultures. We refer to them as white adipocyte cultures 1–3.

We found that these three clonal preadipocyte cell lines, upon differentiation, were highly adipogenic, as assessed by Oil-Red-O staining (Fig. 1a). We further found that after experimentally induced differentiation, brown adipocyte cultures 1–3 showed significantly ($P < 0.001$) higher expression of *UCP1* and *PPARGC1A* (encoding PPAR-γ coactivator 1α) mRNA, both in the basal state and after a 4 h–long treatment with cAMP before harvesting, as compared to white adipocyte cultures 1–3 (Fig. 1b). The *UCP1* mRNA expression in the three brown adipocyte cultures after cAMP treatment was similar to that found in biopsied BAT samples isolated from the supraclavicular region, whereas such induction was not seen in the white adipocyte cultures (Fig. 1b). The induction of *PPARGC1A* expression upon cAMP stimulation in the brown adipocyte cultures, however, did not reach the levels seen in the biopsied BAT control, although it was still potent (Fig. 1b).

UCP1 protein expression was also detected in the three brown adipocyte cultures, but not in the white adipocyte cultures. We observed higher UCP1 expression in brown adipocyte cultures treated with cAMP and rosiglitazonethan in the vehicle-treated cells (Fig. 1c). Notably, the differentiated clonal brown adipocyte cultures showed greater total and uncoupled cellular respiration in both the basal and the cAMP-stimulated states than in the clonal white adipocyte cultures with similar adipogenic properties (Fig. 1d). Induction of greater total and uncoupled cellular respiration was not observed in the brown preadipocyte cell lines (Supplementary Fig. 1c). Furthermore, the differentiated clonal brown adipocyte cultures possessed cAMP-induced lipolysis capacity, as glycerol release was higher in the cells treated with forskolin, a selective activator of the enzyme adenylyl cyclase, as well as in the cells treated with a cell-penetrant cAMP analog, dibutyryl-cAMP than in the vehicle-treated cells (Supplementary Fig. 1d). These data indicate that the three clonal human adipocyte cultures exhibited molecular and functional characteristics of thermogenic adipocytes.

To identify gene signatures that were distinct between human brown and white adipocytes, we employed RNA-seq of clonal brown adipocyte cultures 1–3 and clonal white adipocyte cultures 1–3 (Fig. 2a). A complete list of the genes is provided in Supplementary Table 1. To determine if differentiated human brown adipocytes were similar or different to mouse classical brown adipocytes or beige adipocytes, we overlapped the top 800 differentiated human brown adipocyte–enriched genes with mouse orthologs that were enriched in differentiated classical brown and/or beige adipocytes as previously reported[16] (Fig. 2a). Microarray data sets from clonally derived immortalized mouse beige and classical brown adipocyte cultures under a differentiated state were obtained from the Gene Expression Omnibus (GEO; accession no. GSE39562)[16]. In addition to our own human brown and white adipocyte RNA-seq data sets, we included publicly available microarray data sets of primary differentiated human adipocytes (referred to here as primaries A, B, and C) derived from subcutaneous WAT (GEO accession no. GSE41223; Fig. 2b). Hierarchical clustering revealed that the three differentiated clonal human brown adipocyte cultures belonged to a cluster of mouse beige adipocytes but were distinct from a cluster of mouse classical brown adipocytes (Fig. 2b). As an independent approach, principal component (PC) analysis suggested that the gene-expression profiles of the three differentiated clonal human brown adipocyte cultures were much closer to those of mouse beige adipocytes than to those of mouse classical brown adipocytes (relative Euclidean distance from human brown adipocytes to mouse beige and classical brown adipocytes was 9.4. and 18.1, respectively) (Fig. 2c). These results suggest that the molecular signatures of adult human brown adipocytes resemble those of mouse beige adipocytes rather than mouse classical brown adipocytes.

Of note, RNA-seq analysis of the three clonal human preadipocyte cell lines before differentiation revealed that the molecular signatures of brown and white preadipocytes were distinct and formed separate clusters (Fig. 2d). Consistent with a recent report[23], we found that the expression of contactin-associated protein-like 3 (CNTNAP3), leucine-rich repeat-containing 17 (LRRC17), regulator of G-protein signaling 7 binding protein (RGS7BP), phosphodiesterase 5A, cGMP-specific (PDE5A), and ATP-binding cassette, subfamily A,

member 9 (*ABCA9*) was higher in the clonal brown preadipocyte lines than that in the clonal white preadipocyte lines (Supplementary Table 2). This separation at the gene-expression level was further validated by volcano plot analysis, which showed that the degree of difference in brown and white adipocyte transcriptomes was comparable between undifferentiated and differentiated states (Fig. 2e). These results indicate that the cellular fate of brown versus white adipocytes is largely determined at the precursor cell stage in adult humans.

From a developmental standpoint, it has been reported that mouse beige adipocytes, but not classical brown adipocytes, express smooth muscle lineage–selective genes and that a subset of beige adipocytes arises from smooth muscle myosin, heavy chain 11, (*Myh11*)-positive smooth muscle–like precursors[24]. Indeed, the isolated clonal human brown preadipocyte lines abundantly expressed smooth muscle lineage–selective genes, including *ACTA2, TAGLN, MYL9*, and *CNN1*, the master smooth muscle transcription factor *SRF*, and the non-cardiac co-activator *MKL1* (Supplementary Fig. 2 and Supplementary Table 3). These results further support the possibility that adult human brown adipocytes exhibit beige-like characteristics. The subcutaneous WAT–derived white preadipocyte lines also expressed some of the smooth muscle lineage–selective genes, implying that these cells may also possess 'browning' plasticity given appropriate external stimuli.

To identify human brown adipocyte–selective markers, we analyzed the overlapped gene sets between human and mouse brown adipocyte–enriched genes, which could be classified into four groups. Group A contained genes that were enriched in the differentiated clonal human brown adipocyte cultures as well as in mouse classical brown and beige adipocytes (Fig. 3a). Here we found previously defined BAT markers, such as *UCP1, PPARGC1A, EBF2* (ref. 25), and BMPR1A[26] (Fig. 3b and Supplementary Table 4). The other groups consisted of genes that were enriched in both human brown adipocytes and mouse beige adipocytes (group B), genes enriched in both human brown adipocytes and mouse classical brown adipocytes (group C), and genes enriched only in human brown adipocytes (group D). The subsequent gene ontology (GO) analysis found that the group A gene set was enriched with genes encoding members of the metabolic pathways involved in BAT thermogenesis, such as the electron transport chain, mitochondria biogenesis, cellular respiration, fatty acid oxidation, lipid modification, and acetyl-CoA metabolism (Fig. 3c). Next we validated the expression profiles of 36 representative human brown adipocyte–enriched genes from biopsied human BAT samples[18] and integrated the correlation coefficient among these genes. The correlation analysis found that a large number (31 out of 36; 86.1%) of these genes showed significant ($P < 0.05$) positive correlations in expression (Supplementary Fig. 3a). We further validated the expression of human BAT marker-gene candidates in the differentiated clonal brown and white adipocyte cultures as well as in differentiated primary white adipocytes (Supplementary Fig. 3b). Based on the high correlation coefficient of the new BAT marker–gene candidates with the known BAT markers, the reproducible enrichment in all of the isolated brown adipocyte cultures as well as in human BAT depots from three independent cohorts, and the inducible expression in response to cAMP stimuli and cold temperature, we selected *MTUS1* (encoding mitochondrial tumor suppressor 1) and *KCNK3* (encoding potassium channel, subfamily K,

member 3) as novel human BAT marker genes. *MTUS1* and *KCNK3* showed a highly significant correlation with previously defined BAT marker genes such as *PPARGC1A, PRDM16*, and *CIDEA* (Fig. 3d). Furthermore, *MTUS1* and *KCNK3* expression were significantly higher in UCP1-positive BAT depots than in UCP1-negative WAT depots isolated from the neck regions of the same individuals (eight pairs)[21] (Fig. 3e). Similarly, MTUS1 and KCNK3 proteins were detected in the UCP1-positive BAT depots from the supraclavicular region (Supplementary Fig. 3c). Higher expression of *KCNK3* in human BAT compared to WAT was also validated from two independent data sets[27,28]. Of note, *MTUS1* and *KCNK3* were enriched in the supraclavicular and posterior mediastinum BAT depots but not in the retroperitoneal BAT depots (Supplementary Fig. 3d), indicating that retroperitoneal BAT depots may contain a brown adipocyte population that is distinct from that in the supraclavicular and posterior mediastinum BAT depots in adult humans.

Next we examined the regulatory pathways of *MTUS1* and *KCNK3* in the three differentiated clonal human brown adipocyte cultures and the supraclavicular BAT depots of adult humans. *MTUS1* encodes a mitochondria-localized protein that is known to interact with the C terminus of angiotensin II type 2 receptor and regulate cell proliferation[29]. Among multiple alternatively spliced transcript variants, we found that variant 3 of *MTUS1* was highly responsive to cAMP stimulation in human brown adipocytes (Supplementary Fig. 4a–c). Expression of *KCNK3*, which encodes a pH-dependent, voltage-insensitive potassium channel protein, was also higher in the brown adipocyte cultures treated by forskolin than in the vehicle-treated brown adipocyte cultures (Supplementary Fig. 5a). Importantly, expression of both *MTUS1* variant 3 and *KCNK3* was significantly induced in the supraclavicular BAT depots from six subjects under prolonged cold exposure (19 °C) versus thermoneutral conditions (30 °C)[30] (Fig. 3f). Furthermore, *MTUS1* and *KCNK3* expression exhibited a significant positive correlation with *UCP1* after cold stimuli (Fig. 3g). We also found that mRNA expression of *Mtus1* and *Kcnk3* was higher in the inguinal WAT of mice treated with the beta3-adrenergic receptor agonist CL-316,243 than in that of saline-treated mice (Supplementary Fig. 5b). Such induction was mediated by an increase in intercellular cAMP levels because *MTUS1* and *KCNK3* expression was significantly ($P <$ 0.05) higher in the brown adipocyte cultures treated with either dibutyryl-cAMP or norepinephrine than in those treated with vehicle (Supplementary Fig. 5c). These results suggest that *MTUS1* and *KCNK3* are regulated by the sympathetic nerve–mediated cAMP pathway in mice and humans.

A positive correlation between the new BAT markers and *UCP1* expression suggests possible functional roles of MTUS1 and KCNK3 in beige adipocytes. Because of the close relationship between adult human adipocytes and mouse beige adipocytes, we tested the functional roles of Mtus1 and Kcnk3 in beige adipocytes. To this end, differentiation potential and thermogenic function were tested in beige adipocytes from SVFs of mouse inguinal WAT[17]. These beige adipocytes were transfected with siRNAs targeting *Kcnk3* and *Mtus1* (Fig. 4a). We found that Ucp1 protein expression was substantially lower in the beige adipocytes depleted of *Kcnk3* and *Mtus1* than in the control siRNA-transfected cells (Fig. 4b). Expression of brown and beige adipocyte–selective molecular markers, such as *Ucp1, Cidea* and *Cox7a*, was significantly lower in the cells transfected with siRNAs targeting

Mtus1 and *Kcnk3* than the control siRNA-transfected cells (Fig. 4c). In contrast, knockdown of *Fzd8*, a mouse classical brown adipocyte–enriched gene, did not affect the brown and beige adipocyte–selective gene expression. No significant change was observed in the expression of a general adipogenic marker, adiponectin. Importantly, uncoupled cellular respiration was significantly lower in the cells depleted with *Mtus1* and *Kcnk3* than in the control siRNA-transfected cells upon cAMP stimulation (Fig. 4d). These results indicate that Mtus1 and Kcnk3 are required for beige adipocyte differentiation and thermogenic function.

It should be noted that single-cell cloning inevitably selects highly proliferative cell populations, regardless of biopsied locations and sample numbers. Possible cell-intrinsic changes that occur with obesity or aging await future investigations. While the present data do not exclude the possibility that classical brown adipocytes exist in adult humans, our unbiased global RNA-seq data analyses suggest that adult human BAT from supraclavicular regions displays molecular signatures that resemble beige adipocytes. This is in agreement with previous studies reporting that mouse beige adipocyte–enriched genes are highly expressed in adult human BAT[16,18,19], and that the expression profile of tumor necrosis factor receptor superfamily, member 9 (*TNFRSF9*) clustered with that of *UCP1* in the deeper neck adipose tissue[21]. This view is also supported by recent reports demonstrating that chronic cold acclimation robustly increases BAT mass in the supraclavicular region of adult humans who do not possess detectable BAT before treatment, in parallel with an increase in cold-induced energy expenditure[31,32] or with an improvement in post-prandial insulin sensitivity[33]. The present study together with previous reports[8,16,18,19,31–33] strongly indicates that adult human BAT is recruitable in response to physiological external cues such as chronic cold exposure. This research constitutes an important foundation for future human BAT studies. The isolated cells will provide new opportunities for investigating the cellular mechanisms of human BAT development and could potentially serve as a tool for cell-based disease modeling using CRISPR or TALEN technologies. These cells can also be applied to cell-based small-molecule screenings or unbiased RNAi screenings to identify novel regulators of human BAT thermogenesis. Furthermore, the newly identified genes, *KCNK3* and *MTUS1* variant 3, can serve as molecular markers secondary to *UCP1* for assessing the number of thermogenic adipocytes within human adipose tissues.

ONLINE METHODS

General experimental approaches

No samples, mice or data points were excluded from the reported analyses. Mice were randomly assigned to two groups at the time of purchase to minimize any potential bias. No blinding was applied upon harvesting tissues after the treatment with saline or CL-316,243. RNA-seq and library constructions were performed by technical staff at the UCSF genome core who were blinded to the experimental groups. In other experiments, the investigators were not blinded to group allocation.

Isolation of clonal adipocytes from adult human BAT

Stromal vascular fractions (SVFs) were isolated from supraclavicular adipose tissues from two individuals from whom data were obtained and reported previously[20] (30 and 43 years

old; BMI, 23 and 26 kg/m^2, respectively). Primary white preadipocytes from subcutaneous WAT were obtained from PromoCell (Heidelberg, Germany). SVFs were infected with a retrovirus expressing large T antigen (pBabe SV40 Large T antigen; Addgene) and subsequently selected using puromycin (2 μg/ml). Initially, 23 lines of sub-clonal cells were generated from the supraclavicular biopsies. Subsequently, single cell clones were obtained from the highly adipogenic sub-clonal lines by limiting dilution of cells into 96-well plates (0.2 cells/well). Wells containing cells were trypsinized and propagated in 48-well, 24-well, 12-well, 6-well, 60 mm plates, and finally 100 mm plates. A total of 65 clonal lines were originated from supraclavicular biopsies and screened for adipogenic potential. Similarly, 35 clonal lines were generated using SVFs from subcutaneous WAT with a BMI-matched individual. We obtained seven adipogenic clonal lines from supraclavicular biopsies and six adipogenic clonal lines from subcutaneous WAT. The clonally derived white adipocyte cultures after differentiation were used for Oil-red-O staining in Figure 1a; for mRNA and protein expression analyses in Figures 1b,c and 3a–c and Supplementary Figures 3b, 4b–c, and 5a, for cellular respiration assays in Fig. 1d, and for RNA-seq analyses in Figure 2a–c,e. Undifferentiated clonal white preadipocyte cell lines were used for RNA-seq analyses in Fig. 2d,e, and for cellular respiration assays in Supplementary Figure 1c. Differentiated primary non-clonal adipocytes were used in the gene expression study in Supplementary Figure 3b. As described in detail later, gene expression data of differentiated primary human adipocytes from subcutaneous WAT (human primaries A, B, and C) included in the analysis in Figure 2b were obtained from publically available microarray data sets (Accession: GSE41223).

Cell culture

Human preadipocytes were seeded in collagen-coated plates (BD Biosciences) and cultured in Advanced DMEM/F-12 medium (without phenol red) supplemented with 10% FBS, 50 IU penicillin, and 50 μg/ml streptomycin. When cells reached confluence, adipocyte differentiation was induced with medium containing 10% FBS, 5 μg/ml insulin, 1 nM T3, 0.125 mM indomethacin, 0.2 mM isobutylmethylxanthine (IBMX), and 2 μg/ml dexamethasone for 2 d. Subsequently, the cells were cultured in DMEM/F-12 medium in the presence of insulin, dexamethasone, and T3 for an additional 19 d. For rosiglitazone treatment, cells were treated with 1 μM rosiglitazone during the differentiation. For cAMP treatment, cells were incubated with 10 μM forskolin and harvested after 4 h for RNA isolation and 6 h for protein analysis. For mouse adipocyte culture, primary SVFs were isolated from the inguinal WAT of B6 male mice, according to the methods as previously reported[12,17]. The SVFs were cultured to confluence and adipocyte differentiation was induced with DMEM/F-12 medium (with phenol red) containing 10% FBS, 5 μg/ml insulin, 1 nM T3, 0.25 mM IBMX, 0.125 mM indomethacin, and 2 μg/ml dexamethasone. Two days after induction, cells were switched to the maintenance medium containing 10% FBS, 5 μg/ml insulin, 1 nM T3 for an additional 6 d. To induce beige adipocyte differentiation, cells were differentiated in the presence of rosiglitazone at a dose of 0.5 μM, as outlined in a previous paper[17]. Mycoplasma infections were not tested in the experiments.

RNAi-mediated gene knockdown

For RNAi-mediated gene knockdown, individual siRNA pools for *Mtus1* (no. 065229), *Kcnk3* (no. 043787) and *Fzd8* (no. 045544) were obtained from GE Dharmacon. Non-targeting siRNA (no. 001810; GE Dharmacon) was used as the control. Immortalized preadipocytes derived from SVFs of mouse inguinal WAT were first reverse-transfected with siRNA (25 pmol/0.2×10^6 cells) using Lipofectamine RNAiMAX following the manufacturer's protocol. The cells were forward-transfected 2 d after the first transfection. Cells were differentiated under an adipogenic condition that promotes beige adipocyte differentiation for 4 d (ref. 17). Knockdown of genes was validated by qRT-PCR using the primers listed in Supplementary Table 5.

RNA sequencing (RNA-seq)

RNA-seq libraries were constructed from total RNA using the Ovation RNA-seq system version 2 (NuGEN). The isolated RNA was reverse-transcribed to cDNAs using a combination of random hexameric and a poly-T chimeric primer. The cDNA libraries were subsequently amplified using the Ultralow DR library kit (NuGEN) according to the manufacturer's instructions. Quality of the libraries was validated by Bioanalyzer (Agilent Technologies). Subsequently, high-throughput sequencing was performed using a HiSeq 2500 instrument (Illumina) at the UCSF Genomics Core Facility. Raw reads for each library were mapped using TopHat version 2.0.8 against the indexed human (hg19) or mouse (mm9) genome, downloaded from the TopHat website (http://ccb.jhu.edu/software/tophat/igenomes.shtml). The mapped reads were converted to FPKM (fragments per kilobase of exon per million fragments mapped) by running Cuffdiff 2 (http://cufflinks.cbcb.umd.edu) to determine gene expression[34]. The RNA-seq reads were deposited in ArrayExpress (http://www.ebi.ac.uk/arrayexpress/?) under accession numbers E-MTAB-2602 for human brown and white adipocytes and E-MTAB-2624 for mouse primary brown, beige, and white adipocytes.

Human and mouse transcriptome analyses

To compare human and mouse adipocyte transcriptomes, the gene microarray data sets from mouse beige and classical brown adipocytes were downloaded from Gene Expression Omnibus (GEO) (Accession: GSE39562) as previously reported[16]. Among 13 putative beige cell lines, three lines were used for our bioinformatics analysis since they were functionally validated by oxygen consumption assays, cell transplantation experiments, or UCP1 protein expression by western blotting. The following microarray data were used in the analysis shown in Figure 2: GSM971716 (designated as A), GSM971714 (B), and GSM971698 (C). Microarray data (GSM971717, GSM971718, and GSM971719) were used for mouse classical brown adipocytes and designated as A, B, and C, respectively. In addition to our human brown and white adipocyte RNA-seq data, we included a publically available microarray data set of primary human adipocytes derived from subcutaneous WAT (Accession: GSE41223). All the microarray data sets were normalized by quantile normalization[35] using the dChip Software[36]. To combine the human and mouse data, we used ortholog information downloaded from Ensembl release 75. Clustering analysis was performed using differentially expressed genes (>2-fold) as determined by the comparison

between mouse beige adipocyte lines and mouse classical brown adipocyte lines. FPKM was normalized to array signal in order to set the mean expression level of each gene equal between humans and mice. The top 800 highly expressed genes were used for the clustering analysis in Figure 2b,c. Similar clustering patterns were seen when the top 500, 1,000, 1,500, and 2,000 highly expressed genes or all the genes filtered by variance were subjected to the analyses.

Thirty-six representative human brown adipocyte–enriched genes were identified from the clustering analysis and further selected based on the additional criteria in which mRNA expression levels were high (averaged FPKM > 2.0) in differentiated human brown adipocytes and consistent among the three independent clonal cell lines (relative s.d. of FPFM < 1.0).

Multivariate statistics

Principal component (PC) was computed from the covariance matrix of the human and mouse transcriptome profiles. Hierarchical clustering (HCL) was performed with the complete linkage method using the Pearson correlation as a distance metric. The measured mRNA expressions in RNA-seq were z-scored and visualized as a heat-map representation in the blue-white-red scheme. All statistical analyses were performed using the JMP software version 9 (SAS Institute) or Multi Experiment Viewer[37]. TreeGraph 2 (ref. 38) was used to generate dendrogram trees. Gene Ontology (GO) enrichment analysis was performed in DAVID[39] using the biological process terms (GO FAT category).

Quantitative PCR

Total RNA was isolated using RiboZol reagents (AMRESCO) following the manufacturer's protocol. Quality of the RNA from all samples was validated by a NanoDrop spectrophotometer (Thermo Scientific). Reverse transcription reactions were performed using an iScript cDNA synthesis kit (Bio-Rad). Quantitative reverse transcriptase PCR (qRT–PCR) was performed with SYBR green fluorescent dye using the ViiA 7 Real-Time PCR System (Life Technologies). For the analysis of human BAT (eight pairs)[21], total RNA was extracted from tissues using an RNA MiniPrep kit (Zyme Research) according to the manufacturer's instructions. cDNA was prepared from 2 ng/μl of RNA using the High Capacity cDNA Reverse Transcription kit (Applied Biosystems) according to the manufacturer's instructions. Quantitative RT-PCR assays were run in duplicates and quantified in the ABI Prism 7900 sequence-detection system. Relative mRNA expression was determined by the delta-Ct method using TATA-binding protein (TBP) as an endogenous control. The sequences of primers used in this study are provided in Supplementary Table 5.

Western blotting

Fully differentiated adipocytes were lysed in RIPA buffer (50 mM Tris, pH 7.5, 150 mM NaCl, 1% Triton-X, 10% glycerol, and cOmplete protease inhibitors (Roche)) and total protein lysates (50 μg) were boiled with 4× NuPage LDS loading buffer (Invitrogen), loaded on a 4–15% SDS-PAGE and subsequently transferred onto PVDF membranes. The blots were blocked in 5% milk in Tris-buffered saline with Tween 20 (TBS-T) and incubated

overnight with rabbit anti-UCP-1 (U6382, Sigma or ab10983, Abcam) or mouse anti-β-actin (A3854, Sigma) overnight. For adipose tissues analysis, antibodies for MTUS1 (clone 1C7, Abnova) and KCNK3 (APC-024, Alomone Labs)[40] were used. Light-chain-specific anti-mouse IgG (115-035-174, Jackson ImmunoResearch) was used as a secondary antibody for MTUS1.

Cellular respiration assay

Cells were plated in the gelatin-coated XF24 V7 cell culture microplates (Seahorse Bioscience) and differentiated into adipocytes. Cells were incubated in pre-warmed XF assay medium (pH 7.4) (no. 101022-100; Seahorse Bioscience) supplemented with sodium pyruvate (final concentration: 1.0 mM) and glucose (final: 25 mM) for 1 h. The oxygen consumption rate (OCR) was measured by the XF^e Extracellular Flux Analyzers (Seahorse Biosciences). Cellular respiration was analyzed by using the following perturbation drugs in succession: 1 μM oligomycin, 1 μM FCCP (carbonyl cyanide-*p*-trifluoromethoxyphenylhydrazone) and 1 μM respiratory chain inhibitors (rotenone/antimycin A). The OCR purely attributed to mitochondria was determined by subtracting rotenone/antimycin A–insensitive OCR from total and uncoupled OCR. For cAMP-induced respiration, fully differentiated adipocytes were incubated with 10 μM of forskolin for 20 h. Three independent experiments were performed.

Adipose tissue samples

Human adipose tissue was collected from eight subjects (three females, five males; 49.6 ± 3.7 years) as paired sets of superficial and deep neck tissue, as described previously[21]. BAT samples from multiple depots were collected as described previously[18]. BAT samples from six subjects both under thermoneutral conditions and after prolonged cold exposure at 19 °C were collected as previously reported[30]. As provided in each study, written informed consent was obtained from all individuals or parents/legal guardians in the presence of a witness for each study. The study shown in Figure 3e was approved by the Human Studies Institutional Review Boards of Beth Israel Deaconess Medical Center, Joslin Diabetes Center, and Massachusetts General Hospital[21]. The study shown in Figure 3d and Supplementary Figure 3a,c,d was approved by the Institutional Review Board of Children's Hospital Los Angeles[18]. The study shown in Figure 3f,g was approved by the University of Texas Medical Branch and Institute for Translational Sciences Institutional Review Boards[30].

Animal studies

All animal experiments were performed according to procedures approved by the Institutional Animal Care and Use Committee for animal care and handling at the University of California, San Francisco. 8-week-old male C57BL/6J mice were obtained from the Jackson Laboratory. Mice were randomly assigned to different treatments (saline or CL-316,243) at the time of purchase to minimize any potential bias ($n = 5$ per group). Mice were intraperitoneally injected daily with 0.9% saline or beta3-adrenergic receptor-specific agonist CL-316,243 (Sigma) at a dose of 1 mg/kg for 7 d. Adipose tissues were harvested

for molecular and biochemical analyses. The investigators were not blinded to sample allocation during the experiments.

Statistics

The sample sizes chosen for the experiments were calculated by power analysis ($\alpha = 0.05$ and power of 0.8). The pwr package in the R statistics package, which implements power analysis as outlined by Cohen[41], was used for our sample size determination. Sample size used is specified in each figure legend. Where parametric tests (*t*-test) were used, normal distribution and difference of variance were tested by Shapiro–Wilk test and *F*-test, respectively. When the null hypothesis of equal variance was rejected, Welch's *t*-test was used. Otherwise, Student's *t*-test was used. When normal distribution was not assumed, a nonparametric method (Wilcoxon signed-rank test) was used. Data are expressed as means ±s.e.m. The Pearson correlation and its significance (H_0 = true correlation is equal to 0) were determined by the R statistics package. $P < 0.05$ was considered significant in all the experiments.

Supplementary Material

Refer to Web version on PubMed Central for supplementary material.

ACKNOWLEDGMENTS

References

1. Cypess AM, et al. Identification and importance of brown adipose tissue in adult humans. N. Engl. J. Med. 2009; 360:1509–1517. [PubMed: 19357406]

2. Ouellet V, et al. Outdoor temperature age, sex, body mass index, and diabetic status determine the prevalence, mass, and glucose-uptake activity of 18F-FDG-detected BAT in humans. J. Clin. Endocrinol. Metab. 2011; 96:192–199. [PubMed: 20943785]

3. van Marken Lichtenbelt WD, et al. Cold-activated brown adipose tissue in healthy men. N. Engl. J. Med. 2009; 360:1500–1508. [PubMed: 19357405]

4. Yoneshiro T, et al. Age-related decrease in cold-activated brown adipose tissue and accumulation of body fat in healthy humans. Obesity (Silver Spring). 2011; 19:1755–1760. [PubMed: 21566561]

5. Saito M, et al. High incidence of metabolically active brown adipose tissue in healthy adult humans: effects of cold exposure and adiposity. Diabetes. 2009; 58:1526–1531. [PubMed: 19401428]

6. Nedergaard J, Bengtsson T, Cannon B. Unexpected evidence for active brown adipose tissue in adult humans. Am. J. Physiol. Endocrinol. Metab. 2007; 293:E444–E452. [PubMed: 17473055]

7. Virtanen KA, et al. Functional brown adipose tissue in healthy adults. N. Engl. J. Med. 2009; 360:1518–1525. [PubMed: 19357407]

8. Lidell ME, et al. Evidence for two types of brown adipose tissue in humans. Nat. Med. 2013; 19:631–634. [PubMed: 23603813]

9. Seale P, et al. PRDM16 controls a brown fat/skeletal muscle switch. Nature. 2008; 454:961–967. [PubMed: 18719582]

10. Atit R, et al. Beta-catenin activation is necessary and sufficient to specify the dorsal dermal fate in the mouse. Dev. Biol. 2006; 296:164–176. [PubMed: 16730693]

11. Timmons JA, et al. Myogenic gene expression signature establishes that brown and white adipocytes originate from distinct cell lineages. Proc. Natl. Acad. Sci. USA. 2007; 104:4401–4406. [PubMed: 17360536]

12. Ohno H, Shinoda K, Ohyama K, Sharp LZ, Kajimura S. EHMT1 controls brown adipose cell fate and thermogenesis through the PRDM16 complex. Nature. 2013; 504:163–167. [PubMed: 24196706]

13. Harms M, Seale P. Brown and beige fat: development, function and therapeutic potential. Nat. Med. 2013; 19:1252–1263. [PubMed: 24100998]

14. Kajimura S, Saito M. A new era in brown adipose tissue biology: molecular control of brown fat development and energy homeostasis. Annu. Rev. Physiol. 2014; 76:225–249. [PubMed: 24188710]

15. Waldén TB, Hansen IR, Timmons JA, Cannon B, Nedergaard J. Recruited vs. nonrecruited molecular signatures of brown, "brite," and white adipose tissues. Am. J. Physiol. Endocrinol. Metab. 2012; 302:E19–E31. [PubMed: 21828341]

16. Wu J, et al. Beige adipocytes are a distinct type of thermogenic fat cell in mouse and human. Cell. 2012; 150:366–376. [PubMed: 22796012]

17. Ohno H, Shinoda K, Spiegelman BM, Kajimura S. PPARgamma agonists induce a white-to-brown fat conversion through stabilization of PRDM16 protein. Cell Metab. 2012; 15:395–404. [PubMed: 22405074]

18. Sharp LZ, et al. Human BAT possesses molecular signatures that resemble beige/brite cells. PLoS ONE. 2012; 7:e49452. [PubMed: 23166672]

19. Lee P, Werner CD, Kebebew E, Celi FS. Functional thermogenic beige adipogenesis is inducible in human neck fat. Int. J. Obes. (Lond). 2014; 38:170–176. [PubMed: 23736373]

20. Jespersen NZ, et al. A classical brown adipose tissue mRNA signature partly overlaps with brite in the supraclavicular region of adult humans. Cell Metab. 2013; 17:798–805. [PubMed: 23663743]

21. Cypess AM, et al. Anatomical localization, gene expression profiling and functional characterization of adult human neck brown fat. Nat. Med. 2013; 19:635–639. [PubMed: 23603815]

22. Villarroya F, Vidal-Puig A. Beyond the sympathetic tone: the new brown fat activators. Cell Metab. 2013; 17:638–643. [PubMed: 23583169]

23. Tews D, et al. Comparative gene array analysis of progenitor cells from human paired deep neck and subcutaneous adipose tissue. Mol. Cell. Endocrinol. 2014; 395:41–50. [PubMed: 25102227]

24. Long JZ, et al. A smooth muscle-like origin for beige adipocytes. Cell Metab. 2014; 19:810–820. [PubMed: 24709624]

25. Rajakumari S, et al. EBF2 determines and maintains brown adipocyte identity. Cell Metab. 2013; 17:562–574. [PubMed: 23499423]

26. Schulz TJ, et al. Brown-fat paucity due to impaired BMP signalling induces compensatory browning of white fat. Nature. 2013; 495:379–383. [PubMed: 23485971]

27. Svensson PA, et al. Gene expression in human brown adipose tissue. Int. J. Mol. Med. 2011; 27:227–232. [PubMed: 21125211]

28. Søndergaard E, et al. Chronic adrenergic stimulation induces brown adipose tissue differentiation in visceral adipose tissue. Diabet. Med. 2015; 32:e4–e8. [PubMed: 25252000]

29. Nouet S, et al. Trans-inactivation of receptor tyrosine kinases by novel angiotensin II AT2 receptor-interacting protein, ATIP. J. Biol. Chem. 2004; 279:28989–28997. [PubMed: 15123706]

30. Chondronikola M, et al. Brown adipose tissue improves whole-body glucose homeostasis and insulin sensitivity in humans. Diabetes. 2014; 63:4089–4099. [PubMed: 25056438]

31. van der Lans AA, et al. Cold acclimation recruits human brown fat and increases nonshivering thermogenesis. J. Clin. Invest. 2013; 123:3395–3403. [PubMed: 23867626]

32. Yoneshiro T, et al. Recruited brown adipose tissue as an antiobesity agent in humans. J. Clin. Invest. 2013; 123:3404–3408. [PubMed: 23867622]

33. Lee P, et al. Temperature-acclimated brown adipose tissue modulates insulin sensitivity in humans. Diabetes. 63:3686–3698. [PubMed: 24954193]

34. Trapnell C, et al. Differential analysis of gene regulation at transcript resolution with RNA-seq. Nat. Biotechnol. 2013; 31:46–53. [PubMed: 23222703]

35. Irizarry RA, et al. Exploration, normalization, and summaries of high density oligonucleotide array probe level data. Biostatistics. 2003; 4:249–264. [PubMed: 12925520]

36. Li C, Wong WH. Model-based analysis of oligonucleotide arrays: expression index computation and outlier detection. Proc. Natl. Acad. Sci. USA. 2001; 98:31–36. [PubMed: 11134512]

37. Saeed AI, et al. TM4: a free, open-source system for microarray data management and analysis. Biotechniques. 2003; 34:374–378. [PubMed: 12613259]

38. Stöver BC, Muller KF. TreeGraph 2: combining and visualizing evidence from different phylogenetic analyses. BMC Bioinformatics. 2010; 11:7. [PubMed: 20051126]

39. Huang W, Sherman BT, Lempicki RA. Systematic and integrative analysis of large gene lists using DAVID bioinformatics resources. Nat. Protoc. 2009; 4:44–57. [PubMed: 19131956]

40. Inoue M, Harada K, Matsuoka H, Sata T, Warashina A. Inhibition of TASK1-like channels by muscarinic receptor stimulation in rat adrenal medullary cells. J. Neurochem. 2008; 106:1804–1814. [PubMed: 18554317]

41. Cohen, J. Statistical Power Analysis for the Behavioral Sciences. L. Erlbaum Associates; Hillsdale NJ: 1988.
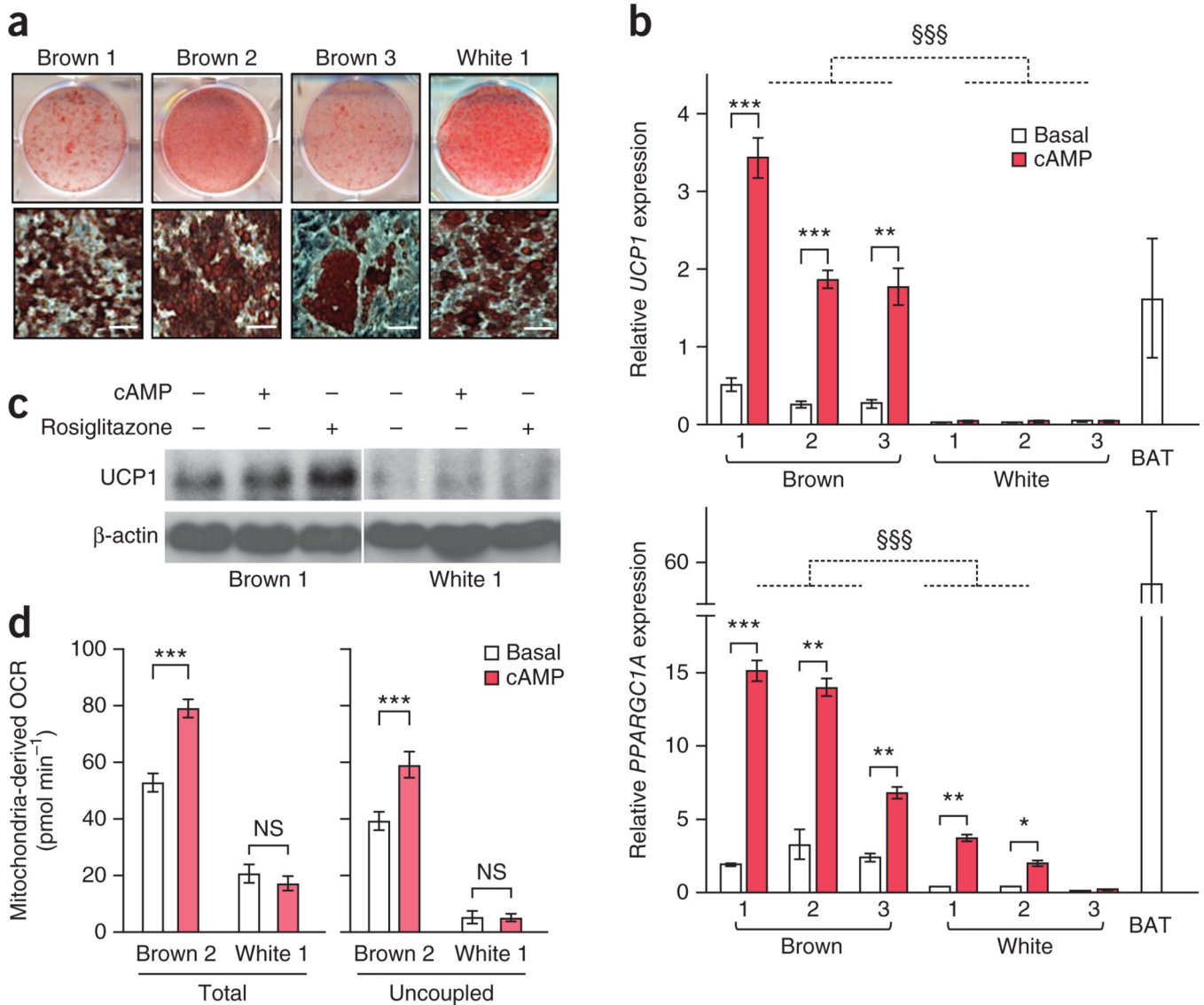
Figure 1.
Isolation of clonal brown adipocytes from adult human BAT. (**a**) Representative Oil-Red-O staining of differentiated brown adipocyte cultures 1–3 and white adipocyte culture 1 at low magnification (top) and at high magnification (bottom). $n = 3$ for all groups. Scale bars, 50 μm. (**b**) Expression of *UCP1* (top) and *PPARGC1A* (bottom) in the differentiated clonal brown adipocyte cultures 1–3 and white adipocyte cultures 1–3 treated with forskolin (cAMP) or vehicle (basal). BAT, biopsied human BAT from the supraclavicular regions (positive control). mRNA expression relative to expression of housekeeping gene TBP. $n = 3$ for all groups. §§§$P < 0.001$, brown versus white adipocyte lines; *$P < 0.05$, **$P < 0.01$, ***$P < 0.001$, brown or white (as indicated) versus basal by one-sided Welch's *t*-test. The error bars for *UCP1* in white adipocytes are 0.001, 0.002 and 0.001 in cultures 1, 2 and 3, respectively. (**c**) Western blot of UCP1 in differentiated brown adipocyte culture 1 and white adipocyte culture 1 treated with forskolin (cAMP) or rosiglitazone. β-actin, loading control. Data are representative of two experiments. (**d**) Total and uncoupled cellular respiration in

differentiated brown adipocyte culture 2 and white adipocyte culture 1 treated with forskolin (cAMP) or vehicle (basal). OCR, oxygen consumption rate. $n = 8$ for all groups. ***$P <$ 0.001 by one-sided Student's t-test. NS, not significant. The variance was similar between basal and cAMP groups ($P = 0.709$). Data are expressed as means $\pm$ s.e.m. for all bar graphs.
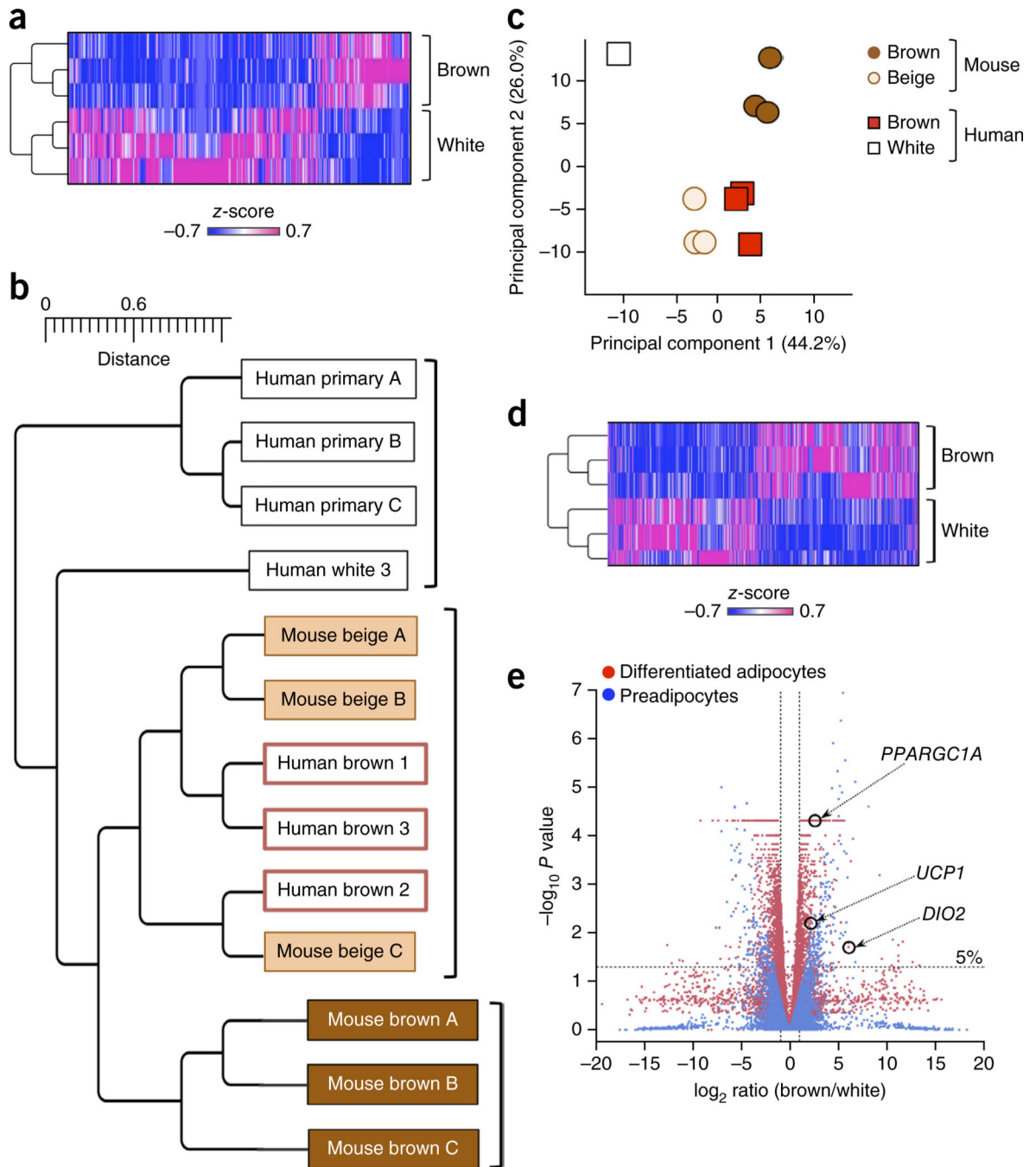
Figure 2.
Genome-wide gene expression analyses indicate a close relationship between human brown adipocytes and mouse beige adipocytes. (**a**) Expression profile and hierarchical clustering of the differentially expressed genes between differentiated clonal human brown adipocyte cultures 1–3 and differentiated clonal white adipocyte cultures 1–3 by two-fold or more. $n = 3$ for each cell type. The color scale shows z-scored FPKM (fragments per kilobase of exon per million fragments mapped) representing the mRNA level of each gene in a blue (low expression)-white-red (high expression) scheme. (**b**) Hierarchical clustering of human and

mouse adipocytes as visualized by TreeGraph. The horizontal distance represents similarities among each cluster. (**c**) Principal component (PC) analysis of the transcriptome from human and mouse differentiated adipocytes. PC analysis was done using the same gene expression data set used in **b**, that is, the RNA-seq data set obtained from differentiated clonal human brown and white adipocyte cultures, and the microarray data set (GSE39562) from differentiated clonal mouse classical brown and beige adipocytes. Numbers in parentheses represent the proportion of data variance explained by each PC. (**d**) Expression profiles and hierarchical clustering of the differentially expressed genes between undifferentiated clonal human brown preadipocyte cell lines 1–3 and white preadipocyte cell lines 1–3 by two-fold or more. $n = 3$ for each cell type. The color scale is the same as in **a**. (**e**) Volcano plot of transcriptomes in the clonal differentiated human brown and white adipocyte cultures (red) and in the clonal undifferentiated human brown and white preadipocyte lines (blue). $n = 3$ for each cell type. The log-fold change between brown versus white is shown on the *x*-axis. The *y*-axis represents the $-\log_{10}$ of the *P* values by delta method–based test. Previously defined BAT-enriched markers are shown.
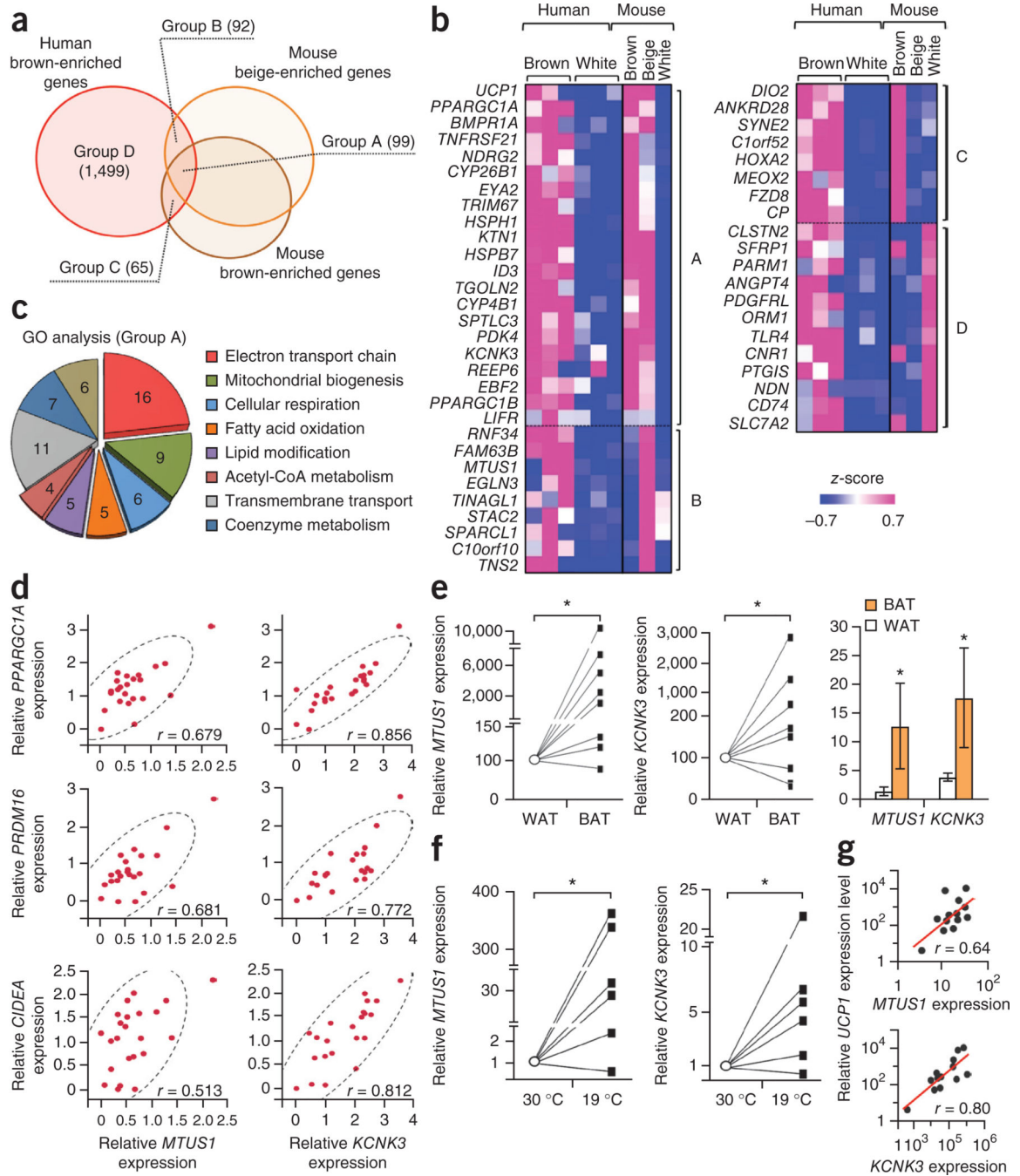
Figure 3.
Identification of human brown adipocyte markers. (**a**) Venn diagram of the overlapping genes enriched in human brown adipocytes, mouse classical brown adipocytes, and mouse beige adipocytes versus white adipocytes of the respective species by two-fold or more. All cells were differentiated clonal adipocytes in culture. $P < 0.05$ by delta method–based test. (**b**) Expression profiles of select genes enriched in each group. The color scale shows z-scored FPKM representing the mRNA level of each gene in blue (low expression)-white-red (high expression) scheme. (**c**) GO analysis of the gene set in Group A (GO FAT category).

The area of each pie slice represents the number of genes that belong to the indicated GO terms. (**d**) Correlation between *MTUS1* and *KCNK3* mRNA expression on the *x*-axis and mRNA expression of previously defined marker genes *PPARGC1A, PRDM16* and *CIDEA* on the *y*-axis. mRNA expression relative to the housekeeping gene TBP. $n = 23$ for each panel. $P < 0.01$ by *z*-test. (**e**) Gene expression of *MTUS1* and *KCNK3* in UCP1-positive adipose tissues (BAT) and UCP1-negative adipose tissues (WAT) from the neck region of the same individuals (eight pairs). *$P = 0.017$ and 0.044, respectively, by Wilcoxon signed-ranked test. The right bar graph shows the expression data without normalization to each individual. Data are expressed as means ± s.e.m. $n = 8$ for each group, *$P < 0.05$ by one-sided Welch's *t*-test. (**f**) mRNA expression of *MTUS1* and *KCNK3* in the supraclavicular BAT isolated from six subjects under thermoneutral conditions (30 °C) and prolonged cold exposure (19 °C). Expression relative to TBP. *$P = 0.035$ and 0.023, respectively, by Wilcoxon signed-ranked test. (**g**) Correlation analysis between *MTUS1* variant 3 or *KCNK3* and *UCP1* under prolonged cold exposure. $n = 13$. $P < 0.01$ by *z*-test.
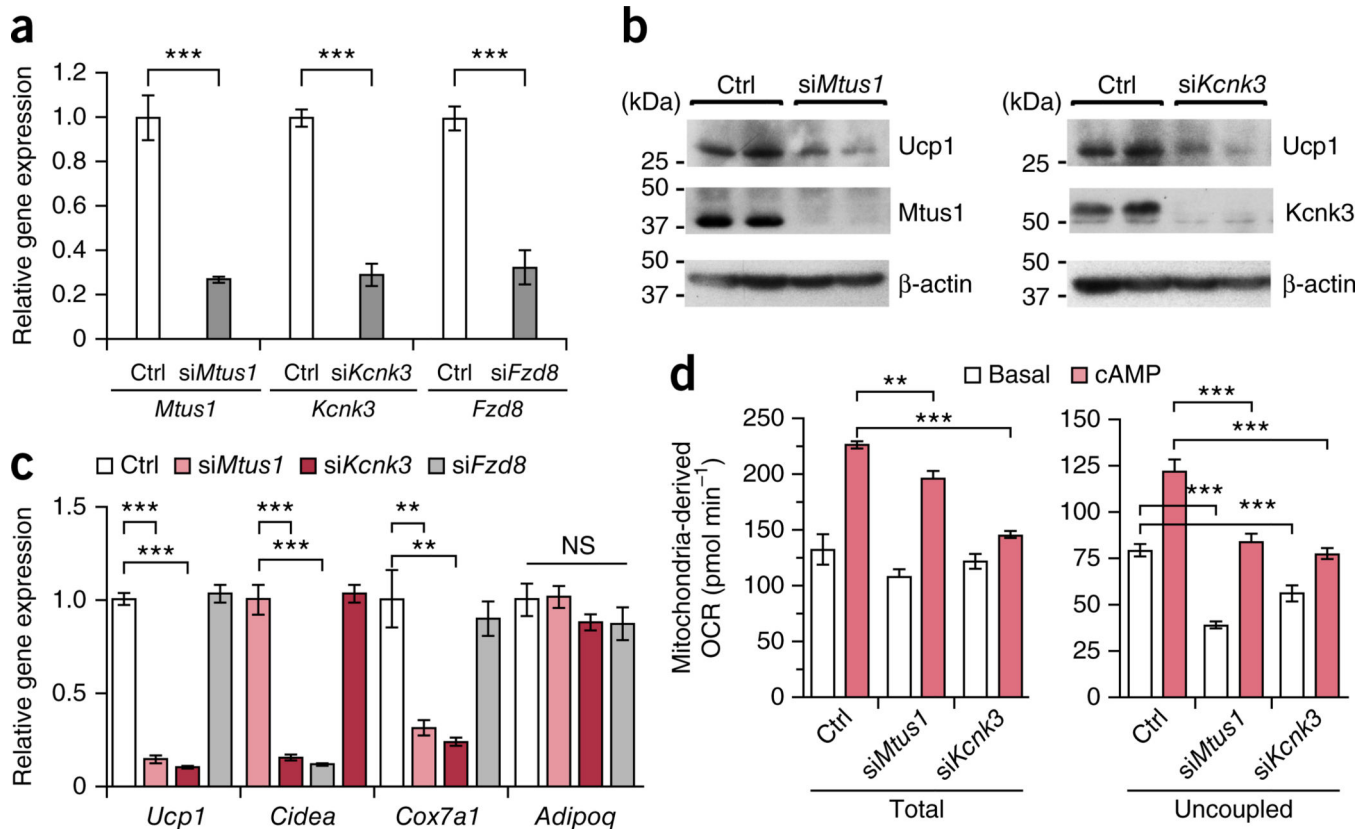
Figure 4.
Mtus1 and Kcnk3 are required for beige adipocyte differentiation and thermogenic function. (**a**) Expression of *Mtus1, Kcnk3*, and *Fzd8* in mouse inguinal WAT-derived adipocytes transfected with siRNAs targeting the indicated genes or non-targeting control (Ctrl). $n = 4$ for all groups. ***$P < 0.001$ for indicated siRNA versus control by one-sided Welch's *t*-test. (**b**) Ucp1, Mtus1 and Kcnk3 protein expression from cells under the same culture condition as in **a**. β-actin, loading control. (**c**) Expression of *Ucp1, Cidea, Cox7a1*, and *Adipoq* (encoding adiponectin) from cells under the same culture condition as in **a**. $n = 4$ for all groups. **$P < 0.01$, ***$P < 0.001$ indicated siRNA versus control by one-sided Student's *t*-test. NS, not significant. (**d**) Total and uncoupled cellular respiration. $n = 8$ for all groups. **$P < 0.01$, ***$P < 0.001$ by one-sided Welch's *t*-test. Data are expressed as means ± s.e.m. for all bar graphs. Data are representative of three independent experiments.